J. Fluid Mech. (2001), *vol.* 443, *pp.* 403–412. Printed in the United Kingdom

Effective pseudo-potentials of hydrodynamic origin

By TODD M. SQUIRES

Department of Physics, Harvard University, Cambridge, MA 02138, USA

(Received 10 April 2001 and in revised form 12 June 2001)

It is shown that low Reynolds number fluid flows can cause suspended particles to respond as though they were in an equilibrium system with an effective potential. This general result follows naturally from the fact that different methods of moving particles in viscous fluids give rise to very different long-range flows. Two examples are discussed: electrophoretic 'levitation' of a heavy charged sphere, for which a hydrodynamic 'pseudo-potential' can be written in closed form, and quasi-two-dimensional crystals of like-charged colloidal spheres which form near charged walls, whose apparent attraction arises not from a force but from persistent fluid flows.

1. Introduction

It is well-known that a particle which is moving under the influence of an external force such as gravity in a viscous fluid sets up a disturbance flow in the fluid which, in the low Reynolds number limit, decays with distance like r^{-1}. The long-range character of these force-driven flows manifests itself in many situations. One example involves collective diffusive behaviour. A pair of Brownian spheres has been predicted (Batchelor 1976) and measured (Crocker 1997) to diffuse in a correlated manner. On the basis of these long-range correlations, Crocker *et al.* (2000) have developed a new technique for the micro-rheology of complex materials. Recently, Dufresne *et al.* (2000) experimentally and theoretically showed the diffusive behaviour of a pair of Brownian spheres to be strongly influenced even by distant solid boundaries. Long-range flows also have a significant influence on the properties of sedimenting systems, giving rise to numerous divergent integrals (see e.g. Hinch 1998). For example, Caflisch & Luke (1985) have predicted velocity fluctuations in sedimenting particulate suspensions to diverge with system size, and Brenner (1999) has drawn attention to the fact that sedimenting particles' long-range interaction with walls can screen the flows and cut off the divergent fluctuations. In addition, long-range hydrodynamic coupling has provided a plausible interpretation (Squires & Brenner 2000) for the experiment of Larsen & Grier (1997), which measured an apparent attraction between like-charged colloidal spheres in the proximity of a similarly charged wall.

It is also well-known that there are other ways to move particles which do not give rise to such long-range disturbance velocity fields. One example is electrophoresis (e.g. Anderson 1989), wherein charged particles move under the influence of an applied electric field. A charged particle in solution attracts oppositely charged counter-ions from the solution, which form a screening 'double-layer' (e.g. Russel, Saville & Schowalter 1989, chap. 4). The particle/double-layer system is electrically neutral, so an applied electric field exerts no net force on the ensemble. However, the charged particle and the counter-ions are driven in opposite directions, giving an apparent

'slip velocity' at the edge of the double layer, and a net motion to the particle. Since velocity fields with r^{-1} decay arise only from a net force on the fluid, electrophoretic (and all force-free) flow fields must decay at least as fast as r^{-2}.

In this paper we will demonstrate that this difference between the long-range disturbance flows due to forced and force-free motions can be exploited to cause particles to behave as though they were subject to equilibrium forces derived from an effective potential. We will use the term 'pseudo-potential' in describing this phenomenon to emphasize that the particle motions arise not from true forces, but from persistent low-Reynolds-number flows which entrain them. This 'pseudo-potential' approach is merely a convenient way to describe and predict particle behaviour, and is not to be understood as representing actual equilibrium properties.

We will explicitly explore two examples of hydrodynamic pseudo-potentials. First, we will discuss the electrophoretic 'levitation' of a heavy charged sphere off a wall, for which an effective pseudo-potential Φ_{ps} can be determined exactly. We will then present a method for making similarly charged colloidal spheres near a wall behave as though there was an apparent attraction between them, so that layered like-charged colloidal crystals can be grown.

We shall first briefly review the hydrodynamics of forced- and force-free motion. Colloidal particles ($\sim 1\,\mu\mathrm{m}$) and their typical velocities ($\sim 1\,\mu\mathrm{m\,s^{-1}}$) are small enough that inertial effects are entirely negligible. In this limit, a rigid sphere of radius a moves due to an external force $\boldsymbol{F}$ at velocity $\boldsymbol{V}_0 = b_0\boldsymbol{F}$, where $b_0 = (6\pi\eta a)^{-1}$ is the Stokes mobility. This motion sets up a disturbance flow in the surrounding fluid

$$\boldsymbol{u}(\boldsymbol{r}) = \frac{1}{8\pi\eta}\left(\frac{\boldsymbol{I}}{R} + \frac{\boldsymbol{RR}}{R^3}\right)\cdot\boldsymbol{F} - \frac{a^2}{24\pi\eta}\left(-\frac{\boldsymbol{I}}{R^3} + \frac{3\boldsymbol{RR}}{R^5}\right)\cdot\boldsymbol{F}, \tag{1.1}$$

where η is the fluid viscosity and $\boldsymbol{R} = \boldsymbol{r} - \boldsymbol{r}_0$ is the vector connecting the observation point $\boldsymbol{r}$ and the centre of the sphere $\boldsymbol{r}_0$. This can be re-expressed using fundamental singularities of the Stokes equation as

$$\boldsymbol{u}(\boldsymbol{r}) = \frac{1}{8\pi\eta}\left\{\boldsymbol{S}(\boldsymbol{R}) - \frac{a^2}{3}\nabla\nabla\cdot\left(\frac{1}{R}\right)\right\}\cdot\boldsymbol{F}. \tag{1.2}$$

The first term represents the flow due to a point force, known as a Stokeslet, which decays like R^{-1}. The second term is the Green's function for a point source dipole, also called a potential dipole, which decays like R^{-3}. The far-field flow is dominated by the Stokeslet, which depends on neither the size nor the velocity of the sphere.

By contrast, a charged insulating sphere with a thin double-layer moving due to a uniform electric field $\boldsymbol{E}_\infty$ sets up a disturbance flow outside the double layer (e.g. Russel *et al.* 1989, p. 256),

$$\boldsymbol{u}_E(\boldsymbol{r}) = \frac{\epsilon\epsilon_0\zeta}{\eta}\frac{a^3}{2}\left(-\frac{\boldsymbol{I}}{R^3} + \frac{3\boldsymbol{RR}}{R^5}\right)\cdot\boldsymbol{E}_\infty, \tag{1.3}$$

where ϵ is the dielectric constant of the fluid and ζ is the potential difference across the double-layer. Here the sphere moves at velocity $\boldsymbol{V}_0 = M_0\boldsymbol{E}_\infty$, where $M_0 = \epsilon\epsilon_0\zeta/\eta$ is the electrophoretic mobility. This flow is exclusively potential dipole flow and decays like R^{-3}. The absence of a Stokeslet R^{-1} decay occurs because there is no net force on the sphere/counter-ion system.

Walls affect these flows significantly, since the fluid velocity must vanish identically on solid boundaries. Image singularities, analogous to image charges in electrostatics, can sometimes be found which exactly cancel a flow set up on the wall. In this paper,

we shall make extensive use of the flow due to a Stokeslet (point force) $F\hat{\boldsymbol{z}}$ oriented perpendicular to a wall, which Blake (1971) found to be

$$\boldsymbol{u}(\boldsymbol{r}) = \frac{F}{8\pi\eta}\left(\boldsymbol{S}(\boldsymbol{R}) - \boldsymbol{S}(\boldsymbol{R}^i) + 2h^2\left\{\nabla_0\nabla_0\left(\frac{1}{R}\right)\right\}\Big|_{\boldsymbol{R}^i} - 2h\left\{\frac{\partial \boldsymbol{S}(\boldsymbol{R})}{\partial z_0}\right\}\Big|_{\boldsymbol{R}^i}\right)\cdot\hat{\boldsymbol{z}}, \tag{1.4}$$

where $\boldsymbol{R}^i = \boldsymbol{R} + 2h\hat{\boldsymbol{z}}$ is the vector between the images and the observation point. In evaluating (1.4), derivatives with respect to the source point $\boldsymbol{r}_0$ (denoted by ∇_0) should be taken first, and then the position $\boldsymbol{R}^i$ inserted in place of $\boldsymbol{R}$. The flow due to the images decays like R^{-1}, whereas the image flow for a source dipole (Blake & Chwang 1974), which will not be required in this paper, decays like R^{-3}.

The velocity of a sphere forced toward a wall has two contributions: it moves at $\boldsymbol{U}_0$ due to the applied force, and to $O(a)$ it is advected at the local fluid velocity due to the flow set up by the image singularities. This advection velocity is obtained by evaluating the image flow from (1.4) at r_0, resulting in an $O(a/h)$ wall correction to the (scalar) mobility for motion perpendicular to the wall (e.g. Happel & Brenner 1983):

$$b_\perp(h) = b_0\left(1 - \frac{9a}{8h} + O\left[\frac{a^3}{h^3}\right]\right). \tag{1.5}$$

The correction to the electrophoretic mobility can be derived in similar fashion, but is slightly more complicated because the wall gives both hydrodynamic and electrostatic contributions. Since the image flow (and electrostatic image potential) for electrophoretic motion decays like R^{-3}, the wall correction to the electrophoretic mobility is $O(a^3/h^3)$, and has been calculated by Keh & Anderson (1985) to be

$$M_\perp(h) = M_0\left(1 - \frac{5a^3}{8h^3} + O\left[\frac{a^5}{h^5}\right]\right). \tag{1.6}$$

In this paper, we treat a/h and a/r as small, and neglect this $O(a^3/h^3)$ variation.

2. Electrophoretic 'levitation'

These two motions and their respective flows can be superposed, since Stokes flow is linear. A charged sphere which sediments due to a force F_g towards a planar electrode and which is electrophoretically driven upwards due to a uniform electric field $\boldsymbol{E}_\infty$ will have a velocity v given by

$$v = -b_\perp(h)F_g + M_\perp(h)E_\infty, \tag{2.1}$$

with $b_\perp(h)$ and $M_\perp(h)$ given by (1.5) and (1.6) respectively. If the bulk electrophoretic velocity is less than the bulk sedimentation velocity, so that $\psi = M_0E_\infty/b_0F_g < 1$, there will be a unique height

$$\frac{h_0}{a} = \frac{9}{8(1-\psi)} + O(a^2) \tag{2.2}$$

where the two velocities exactly balance and a non-Brownian sphere will come to rest. A sphere started above h_0 falls faster than electrophoresis drives it up, and it moves down towards the plane. Similarly, a sphere below h_0 falls too slowly, and electrophoresis drives it up. Thus h_0 is a stable steady location. On the other hand, h_0 would be an unstable steady point for a sphere falling away from a wall.

Such a sphere undergoing Brownian motion has a probability distribution $P(h)$ of being located at h which is given by the steady Fokker–Planck equation (see for

example Batchelor 1977)

$$\frac{\partial P}{\partial t} = 0 = -\frac{\partial}{\partial h}\left[v(h)P - D_\perp(h)\frac{\partial P}{\partial h}\right], \tag{2.3}$$

where $D_\perp = k_\mathrm{B}T b_\perp(h)$ is the diffusion constant. This equation has solution $P(h) = P_0 \exp(-\Phi_\mathrm{ps}/k_B T)$, where Φ_ps is a non-equilibrium 'pseudo-potential'

$$\Phi_\mathrm{ps}(h) = F_\mathrm{g}h - \int^h \frac{M_\perp(h')E_\infty}{b_\perp(h')}\mathrm{d}h'. \tag{2.4}$$

Inserting the values of $b_\perp$ and $M_\perp$ from (1.5) and (1.6) and keeping terms to $O(a/h)$, we integrate (2.4) to obtain

$$\Phi_\mathrm{ps}(h) \approx F_\mathrm{g}h - (M_0 E_\infty/b_0)\left[h + \tfrac{9}{8}a\,\ln\left(h/a - \tfrac{9}{8}\right)\right], \tag{2.5}$$

which can be expanded about h_0 to give an approximately harmonic well

$$\frac{\Phi_\mathrm{ps}}{k_B T} \sim \frac{8}{9}\frac{F_\mathrm{g}a}{k_B T}\left[\frac{(1-\psi)^2}{\psi}\right]\frac{(h-h_0)^2}{2a^2} + \frac{\Phi_\mathrm{ps}(h_0)}{k_B T}. \tag{2.6}$$

If one viewed only the motion of a single sphere in this configuration, without examining the persistent flow around it, one would not be able to distinguish between this non-equilibrium pseudo-potential and a true thermodynamic potential. However, the physical distinction is crucial: the *only* force on the sphere/double-layer system is F_g, directed toward the wall. The extraction of forces from the observed motions of colloidal particles is therefore not unambiguous.

3. Multi-particle pseudo-potential interactions

Even though the electrophoretically 'levitated' particle is stationary, it drives a long-range flow, since the flows due to the forced and force-free motions are different. Far from the sphere, the flow is always dominated by the force-driven motion, since it decays the most slowly. Streamlines for the flow around a hovering sphere, described in § 2, are shown in figure 1(*a*).

A second identical sphere, placed at the same height and at some distance r away from the original sphere, will both set up a long-range flow and be entrained by the flow set up by the first sphere. Forcing two spheres perpendicular to the wall induces a relative velocity between them (Dufresne *et al.* 2000), in the plane of the wall, as is evident from the streamlines in figure 1(*a*). This relative velocity of sphere 1 arises from its entrainment in the flow set up by the images of sphere 2. It can be found to $O(a/h)$ and $O(a/r)$ by evaluating the disturbance flow of sphere 2, given by (1.4), at the position of sphere 1, so that $\boldsymbol{R} = -r\hat{\boldsymbol{x}}$ and $\boldsymbol{R}_\mathrm{i} = -r\hat{\boldsymbol{x}} + 2h\hat{\boldsymbol{y}}$. The advection velocity of sphere 1 is then found to be

$$\dot{x}_1 = -\dot{x}_2 = -\frac{3}{2\pi\eta}\frac{rh^3}{(r^2+4h^2)^{5/2}}F_\mathrm{g}, \tag{3.1}$$

where x is the coordinate parallel to the wall, along the line joining the spheres, as in figure 1(*b*). Two spheres forced away from a wall move together as they leave it, whereas two spheres falling towards a wall move apart. The relative motion between two non-Brownian hovering spheres resembles the motion due to a repulsive force between them, even though it does not arise from a force. Example trajectories for two such spheres are shown by the solid curves in figure 1(*b*), with arrows showing the collapse onto these trajectories from various initial configurations.

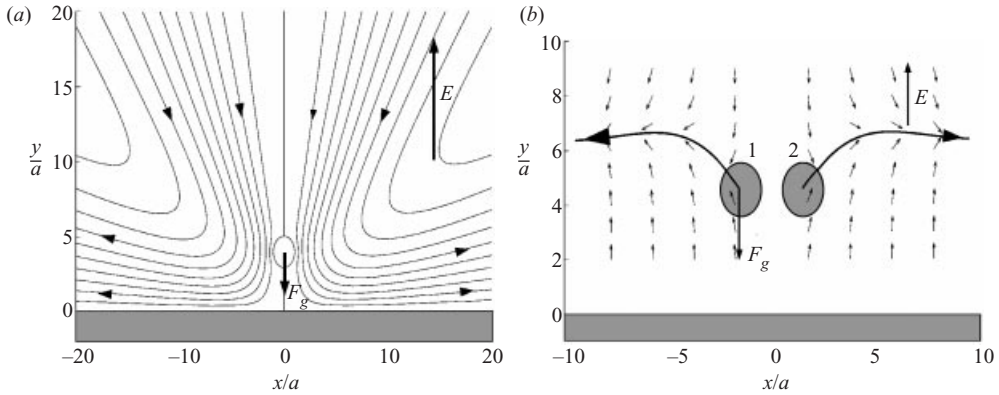

FIGURE 1. (*a*) Streamlines for a heavy charged sphere electrophoretically levitated at $h_0 = 4a$. Flows move down and radially out along the streamlines. The closed streamline shows the slip velocity on the sphere surface. The flow decays slowly and asymptotically approaches the flow due to a falling sphere near a wall, even though the sphere is immobile. (*b*) Two heavy spheres electrophoretically driven upwards approach a stable trajectory, on which the spheres move apart. This mimics a repulsion between the spheres, and asymptotes to two spheres 'hovering' independently. Here E is chosen so that an independent sphere would hover at $h_0 = 6a$.

4. Like-charge colloidal crystal formation

Finally, we explore the possibility of setting up an attractive pseudo-interaction between the spheres, which can lead to crystal formation. In the last section, we demonstrated that two spheres forced toward a wall experience relative motion apart. Combining forced motion *away* from a wall with force-free motion *towards* it will drive the particles together. The simplest way to do this – electrophoretically driving heavy spheres towards a 'ceiling' – will not work, as h_0 is then an unstable point.

Instead, we consider neutrally buoyant charged spheres, and electrophoretically drive them towards a charged wall. This would require a wall which carries a static surface charge, in addition to passing a current. Electrophoresis provides the force-free motion and the sphere's electrostatic and osmotic repulsion from the charged wall provides the forced motion. The fact that electrophoretic motion is force-free, while electrostatic repulsion is forced, is a rather subtle point. In electrophoresis, counter-ions are driven by a tangential electric field along the particle surface, so that a net current flows in the double layer. Thus counter-ions enter the double layer from the bulk solution at one 'pole', travel along the particle surface, then leave the double layer at the other pole – continually lowering their free energy by doing so. By contrast, in the electrostatic interaction, the counter-ions in the sphere's double layer remain there. They feel an electrostatic attraction towards the wall; however, they also feel an osmotic (entropic) repulsion away from it. Because the wall's double layer is already completely charged, there is no 'room' for the sphere's counter-ions, and the sphere/counter-ion system moves as a unit.

The net force F_w on the sphere/counter-ion system near a charged wall is calculated by integrating an electrostatic and osmotic stress tensor over a surface enclosing the sphere and its counter-ions (see e.g. Russel *et al.* 1989, chap. 4). Under the linear superposition approximation, the force the wall exerts on the sphere/counter-ion system is given by

$$\frac{F_w}{k_B T} = 4\pi Z \sigma_g \lambda_B \frac{e^{\kappa a}}{1+\kappa a} e^{-\kappa h}, \tag{4.1}$$

where Z is the effective charge on the sphere, σ_g is the charge density on the wall, κ^{-1} is the Debye screening length and λ_B is the Bjerrum length (≈ 0.7 nm in water at room temperature). This force sets up a flow around each sphere like in figure 1(*a*), with flow arrows reversed. The lateral component of the flow now draws the spheres together. They come together until stopped by their mutual electrostatic repulsion, which is described by pair potential Φ_s,

$$\frac{\Phi_s}{k_B T} = Z^2 \lambda_B \left(\frac{e^{\kappa a}}{1+\kappa a} \right)^2 \frac{e^{-\kappa r}}{r}. \tag{4.2}$$

In the numerical examples which follow, we will use the values $Z = 7300$, $\kappa^{-1} = 0.275\,\mu$m and $2a = 0.652\,\mu$m as in the work of Larsen & Grier (1997). Their article presents two experiments which were presumed related: (i) metastable like-charged colloidal crystallites were observed which were postulated to result from an unexplained wall-mediated attractive force, and (ii) a non-equilibrium measurement of this proposed force was performed, and the consistency of the two results was argued. Squires & Brenner (2000) demonstrated that hydrodynamics alone can account for the 'force' measurement, claiming that the experiment measured relative motion, and interpreted it as force-driven. One unmeasured parameter – the charge density on the wall – was required, and $\sigma_g = 0.4\sigma_s$ was found as the best fit. We choose these values for the present study because the effects under discussion are most pronounced with long screening lengths and high surface charge densities, so that the spheres tend to 'hover' at an appreciable distance from the wall, and also because these effects may bear some relation to the observed metastable crystallites.

The steady-state probability distribution of two such spheres is found using the generalization of (2.3),

$$-\nabla \cdot \boldsymbol{J} = 0 = -\nabla \cdot \{ \boldsymbol{V} P - k_B T \boldsymbol{b} \cdot \nabla P \}, \tag{4.3}$$

where $\boldsymbol{V} = (\boldsymbol{v}_1, \boldsymbol{v}_2)$ is a two-sphere velocity vector, $\boldsymbol{b}$ is the two-sphere mobility tensor, and both depend on $\{h_1, h_2, r\}$. The velocity is given by $\boldsymbol{V} = \boldsymbol{V}_e - \boldsymbol{b} \cdot \nabla \Phi$, where Φ gives the wall–sphere and sphere–sphere potentials and $\boldsymbol{V}_e$ is the electrophoretic velocity.

The probability distribution can be found perturbatively by expanding (4.3) about the stationary point $\{h_0, h_0, r\}$ where $\boldsymbol{V}_e = \boldsymbol{b} \cdot (\nabla \Phi)$. We present instead a more intuitive approximate derivation, justified *a posteriori* by simulations. We expect the spheres will be roughly confined near the height h_0 (whose weak dependence on r we neglect), and assume that height fluctuations will have a negligible effect on the mobility tensor. The spheres then move towards each other with velocity $\dot{x}_1 = -\dot{x}_2$ given by

$$\dot{x}_1 = (b_{x_1 x_1} - b_{x_1 x_2}) |F_p(r)| + b_{x_1 z_2} F_w, \tag{4.4}$$

where $b_{x_1 z_2}$ is the coefficient of $\boldsymbol{b}$ giving the mobility of sphere 1 in the $\hat{\boldsymbol{x}}$-direction due to a force on sphere 2 in the $\hat{\boldsymbol{z}}$-direction, and so on. Were this velocity to arise from a force $|F_{ps}|$ between the spheres, that force would approximately obey

$$\dot{x}_1 \approx (b_{x_1 x_1} - b_{x_1 x_2}) |F_{ps}|. \tag{4.5}$$

These two can be combined to give an approximate form for the pseudo-force

$$F_{ps} \approx F_s + \frac{b_{x_1 z_2} F_w}{b_{x_1 x_1} - b_{x_1 x_2}} \tag{4.6}$$

which contains the true force F_s and the hydrodynamic impostor. Using (1.4) to

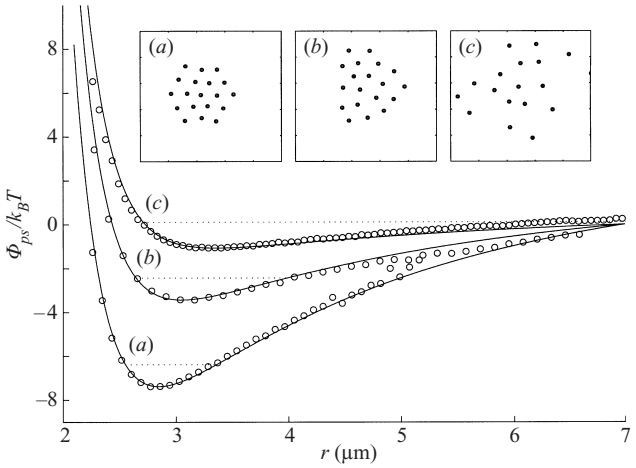

FIGURE 2. Radial pseudo-potentials and representative 'phases' of neutrally buoyant charged spheres electrophoretically driven into the double-layer surrounding a charged wall. (*a*) A strong field ($E_a = 3.3\,\mathrm{V\,cm^{-1}}$, $h_0 = 2\,\mu\mathrm{m}$) yields a deep pseudo-potential well and tight pairwise confinement, giving a regular triangular lattice. (*b*) A moderate field ($E_b = 1.7\,\mathrm{V\,cm^{-1}}$, $h_0 = 2.2\,\mu\mathrm{m}$) yields a pseudo-potential well deep enough to yield a dense phase, but not strong enough to retain orientational order. (*c*) A weak field ($E_c = 0.56\,\mathrm{V\,cm^{-1}}$, $h_0 = 2.5\,\mu\mathrm{m}$) yields an isotropic 'gas'. Dotted lines represent $1k_BT$ of energy and give typical excursions about the equilibrium point. Lines give the approximate analytic form (4.8), and circles give the simulated pseudo-potentials.

evaluate $b_{x_1z_2}$, this can be integrated to yield an approximate pseudo-potential

$$\Phi_{\mathrm{ps}}(r,h_0) \approx \Phi_{\mathrm{s}}(r) - \frac{3h_0^3F_{\mathrm{w}}(h_0)}{2\pi\eta}\int^r \frac{r(4h_0^2+r^2)^{-5/2}}{b_{x_1x_1}(h_0)-b_{x_1x_2}(r,h_0)}\mathrm{d}r, \tag{4.7}$$

where Φ_{s} is the pair potential between the spheres, given by (4.2). Although $b_{x_1x_2}$ is $O(a)$, in practice it is small compared to the $O(a)$ term in $b_{x_1x_1}$, and its neglect allows the direct integration of (4.7) to give

$$\Phi_{\mathrm{ps}}(r,h_0) \approx \Phi_{\mathrm{s}}(r) - \frac{F_{\mathrm{w}}(h_0)}{1-(9a/16h_0)}\frac{3h_0^3a}{(4h_0^2+r^2)^{3/2}}. \tag{4.8}$$

A comparison betweeen (4.8) and simulated results is shown in figure 2, which suggests the approximations are appropriate for these parameters. We simulate the dynamical equations $\boldsymbol{V} = \boldsymbol{b}\cdot\boldsymbol{F} + \boldsymbol{M}\cdot\boldsymbol{E}$, where $\boldsymbol{V}$, $\boldsymbol{b}$ etc. are multiparticle quantities. Brownian motion is accounted for in standard fashion (Ermak & McCammon 1978, Grassia, Hinch & Nitsche 1995), wherein $\boldsymbol{D} = k_BT\boldsymbol{b}$ is a position-dependent tensor diffusivity. The pair correlation function $g(r)$ was calculated from simulations of a pair of spheres and pseudo-potentials Φ_{ps}/k_BT are given by $-\log g(r)$. Unlike the lower two pseudo-potential wells (*a*) and (*b*), the shallowest pseudo-potential well (*c*) is not deep enough for bound states. Simulated pairs of spheres thus wander apart, preventing adequate sampling of the region near the pseudo-potential minimum. We therefore used the method described by Crocker & Grier (1996) to determine the shallowest potential well (*c*).

Equation (4.8) is identical to that derived by Squires & Brenner (2000) in their analysis of the experiment of Larsen & Grier (1997) which measured the effective interaction between like-charged colloidal spheres near a single charged wall. Although the two formulae were derived in the same fashion, they have very different physical consequences. In that experiment, no force-free motion was present. Instead, a pair

of spheres was repeatedly released from the same height h_0, its relative displacement measured, and was then re-trapped; therefore, a net force systematically drove the spheres away from the wall throughout the experiment. Consequently, there was a systematic relative motion of the spheres which had been interpreted to arise from an attractive force. In a steady state system, where the spheres would fluctuate toward the wall as often as away, and furthermore, where they would not be 'pinned' near the wall, one would expect no systematic relative motion, and this hydrodynamic effect would be of no physical consequence.

In the present situation, however, similarly charged spheres in steady state actually do behave as though there was an attraction. Electrophoresis effectively 'pins' the spheres at some height without applying a force, so that the long-range flow which entrains nearby spheres is dominated by the forced motion. A collection of spheres can thus aggregate to form clusters – a behaviour which might otherwise seem to arise from an attractive force. While the former case involves a relative motion which was interpreted to be force-driven but would not act like it in steady state, the present case has a hydrodynamic impostor which does behave like a force in steady state.

We have run simulations which account for Brownian motion to demonstrate that spheres can indeed self-assemble into a quasi-two-dimensional crystal. We retain terms up to $O(a)$ in $\boldsymbol{b}$ and $\boldsymbol{M}$ and use a box of side $100a$ with periodic boundaries. We started nineteen spheres in a hexagonal crystal, then simulated their dynamics until it was clear that the qualitative features would not change. This typically corresponded to approximately a minute of real time. Figure 2 shows the resulting suspensions at the end of each run for three different field strengths. The strongest field, $E_a = 3.3\,\mathrm{V\,cm^{-1}}$ for which $h_0 = 2\,\mu\mathrm{m}$, yields a hexagonal crystal, whereas a weaker field, $E_b = 1.7\,\mathrm{V\,cm^{-1}}$, for which $h_0 = 2.2\,\mu\mathrm{m}$, is strong enough to yield a dense phase, but not strong enough to retain orientational order. We loosely term this an isotropic 'liquid' phase. Finally, for an even weaker field $E_c = 0.56\,\mathrm{V\,cm^{-1}}$, for which $h_0 = 2.5\,\mu\mathrm{m}$, the pseudo-attraction is sufficiently weak that the spheres spread out to fill the box as an isotropic 'gas'. Experimentally, one could study the freezing and melting of these crystals by simply adjusting E_∞ during an experiment, thereby changing h_0, $F_\mathrm{w}(h_0)$, and the strength of the pseudo-attraction.

Finally, we note that there is a persistent non-zero probability current $\boldsymbol{J}$ in the steady state. The probability current can only be zero when

$$-\nabla\Phi_\mathrm{ps} = \boldsymbol{b}^{-1}\cdot\boldsymbol{V} \tag{4.9}$$

has a solution. In equilibrium systems, $\boldsymbol{V} = \boldsymbol{b}\cdot\boldsymbol{F}$ so that $\boldsymbol{F} = -\nabla\Phi_\mathrm{ps}$ as expected. Here $\boldsymbol{V} = \boldsymbol{b}\cdot\boldsymbol{F} + \boldsymbol{V}_E$, and (4.9) will not in general have a solution. Physically, this is because the equivalent pseudo-force required to give velocity $\boldsymbol{V}_E$ would be non-conservative. Vertical fluctuations take the pair into regions of stronger or weaker pseudo-attraction, leading to persistent closed orbits of $\boldsymbol{J}$. The size of the fluctuations about h_0 thus determine the strength of $\boldsymbol{J}$. In our treatment, as in most easily conceivable experiments, we concern ourselves only with the relative separation r between spheres – effectively integrating $P(h_1, h_2, r)$ over heights h_1 and h_2. Thus $\boldsymbol{J}$ plays little role in this study, as confirmed by the comparison between simulations and the analytic approximation (4.8) in figure 2.

5. Discussion and conclusions

While we have specifically investigated the combination of electrophoretically-driven motion and body-force motion, the present results have a wider validity. They

will hold whenever motion using body forces such as gravity, electrostatic repulsion or attraction, magnetic forces, etc. are combined with force-free motion. There are many ways to achieve the latter. Since any self-propelled motion cannot result in a net force or torque on the system, all swimmers generate flows decaying faster than r^{-1} (Lighthill 1976). There are also other types of 'phoretic' motion, which involve particle motion due to fields which interact with the particle's surface (e.g. Anderson 1989), such as thermophoresis (motion due to thermal gradients) and diffusophoresis (motion due to solute concentration gradients). Similarly, the thermocapillary motion of bubbles (Young, Goldstein & Block 1959), driven by thermal surface tension gradients, is force-free.

Having shown that like-charged colloidal crystals can self-assemble into ordered crystals due to long-range persistent non-equilibrium hydrodynamic flows, it is natural to ask whether there could be any connection between these crystals and those observed by Larsen & Grier (1997). These metastable crystallites formed near the charged glass walls of the experimental cells due to an AC electric field oriented parallel to the walls. When the driving field was turned off, they persisted for times orders of magnitude longer than purely repulsive Brownian spheres should. This response can certainly be understood within the present picture, and would require a force-free motion to drive the spheres into the charge cloud of the walls. A spurious current in the cell could do this; however, it is unlikely that this explains Larsen & Grier's crystals, for two reasons: (i) there are no electrodes on the top and bottom walls of their cells, and (ii) the crystals were observed to form on both the top and bottom walls, whereas a net current in the cell would probably drive the spheres to one wall or the other. Since the crystallites were observed immediately after the system was driven with electric fields, one possibility is that some force-free motion arose during the sample cell's re-equilibration. A current, as discussed above, would need to be fairly large – the bulk current densities in figure 2(*a–c*) are 19 000, 9500 and 3300 $\mathrm{e\,s^{-1}\,\mu^{-2}}$ respectively. These are rather large, given that the surface charge density is of order 2000 $\mathrm{e\,\mu^{-2}}$. Other possible mechanisms for force-free motion include thermal or electrolyte concentration gradients; however, it is not clear which if any of these mechanisms are present or responsible for the crystals. It is generally believed that a novel long-ranged attraction between confined like-charged colloids, whose origin remains controversial, gives rise to this behaviour (e.g. Hansen & Lowen 2000). The present work provides a non-equilibrium mechanism whose origins are understood which would mimic an attractive interaction and could drive like-charge colloidal crystallization, so its potential role should be investigated further.

Two-dimensional colloidal crystals have been formed on electrodes via electrophoretic deposition (Bohmer 1996, Trau, Saville & Aksay 1997), and Solomentsev, Bohmer & Anderson (1997) have proposed an electrohydrodynamic model, which bears some similarity to the present work, for its explanation. The difference between our work and that of Solomentsev *et al.* (1997) is that in the latter, the particles are first deposited on the electrode, and then electro-osmotic flows drive adjacent particles towards one another. These flows are much shorter-ranged than the flows described here, and are highly screened due to the close proximity of the wall.

In conclusion, we have used the difference in flow fields set up by force-driven motion and force-free motion to show that persistent long-range viscous flow fields can be set up, resulting in particle motion which mimics an effective potential. This appears surprising at first, since the system is out of equilibrium, and yet behaves as though it is an equilibrium system with an effective potential which is

hydrodynamically driven. Given the general nature of this effect, these persistent flow fields are likely to find various applications in self-assembly and microfluidic contexts.

This work was supported under the NSF Division of Mathematical Sciences grant DMS-9733030.

REFERENCES

Anderson, J. L. 1989 Colloid transport by interfacial forces. *Ann. Rev. Fluid Mech.* **21**, 61–99.

Batchelor, G. K. 1976 Brownian diffusion of particles with hydrodynamic interaction. *J. Fluid Mech.* **74**, 1–29.

Batchelor, G. K. 1977 Developments in microhydrodynamics. In *Theoretical and Applied Mechanics* (ed. W. T. Koiter), pp. 33–55. North Holland.

Blake, J. R. 1971 A note on the image system for a stokeslet in a no-slip boundary. *Proc. Camb. Phil. Soc.* **70**, 303–310.

Blake, J. R. & Chwang, A. T. 1974 Fundamental singularities of viscous flow. 1. Image systems in the vicinity of a stationary no-slip boundary. *J. Engng Maths* **8**, 23–29.

Bohmer, M. 1996 In situ observation of 2-dimensional clustering during electrophoretic depositoin. *Langmuir* **12**, 5747–5750.

Brenner, M. P. 1999 Screening mechanisms in sedimentation. *Phys. Fluids* **11**, 754–772.

Caflisch, R. E. & Luke, J. H. C. 1985 Variance in the sedimentation speed of a suspension. *Phys. Fluids* **28**, 759–760.

Crocker, J. C. 1997 Measurement of the hydrodynamic corrections to the Brownian motion of two colloidal spheres. *J. Chem. Phys.* **106**, 2837–2840.

Crocker, J. C. & Grier, D. G. 1996 Methods of digital video microscopy for colloidal studies. *J. Colloid Interface Sci.* **179**, 298–310.

Crocker, J. C., Valentine, M. T., Weeks, E. R., Gisler, T., Kaplan, P. D., Yodh, A. G. & Weitz, D. A. 2000 Two-point microrheology of inhomogeneous soft materials. *Phys. Rev. Lett.* **85**, 888–891.

Dufresne, E. R., Squires, T. M., Brenner, M. P. & Grier, D. G. 2000 Hydrodynamic coupling of two Brownian spheres to a planar surface. *Phys. Rev. Lett.* **85**, 3317–3320.

Ermak, D. L. & McCammon, J. A. 1978 Brownian dynamics with hydrodynamic interactions. *J. Chem. Phys.* **69**, 1352–1360.

Grassia, P. S., Hinch, E. J. & Nitsche, L. C. 1995 Computer simulations of Brownian motion of complex systems. *J. Fluid Mech.* **282**, 373–403.

Hansen, J. P. & Lowen, H. 2000 Effective interactions between electric double layers. *Ann. Rev. Phys. Chem.* **51**, 209–242.

Happel, J. & Brenner, H. 1983 *Low Reynolds Number Hydrodynamics.* Martinus Nijhoff.

Hinch, E. J. 1988 Sedimentation of small particles. In *Disorder and Mixing* (ed. E. Guyon, J.-P. Nadal & Y. Pomeau), pp. 153–161. Kluwer.

Keh, H. J. & Anderson, J. L. 1985 Boundary effects on electrophoretic motion of colloidal spheres. *J. Fluid Mech.* **153**, 417–439.

Larsen, A. E. & Grier, D. G. 1997 Like-charge attractions in metastable colloidal crystallites. *Nature* **385**, 230–233.

Lighthill, J. 1976 Flagellar hydrodynamics. *SIAM Rev.* **18**, 161–230.

Russel, W. B., Saville, D. A. & Schowalter, W. R. 1989 *Colloidal Dispersions.* Cambridge University Press.

Solomentsev, Y., Bohmer, M. & Anderson, J. L. 1997 Particle clustering and pattern formation during electrophoretic depositions: a hydrodynamic model. *Langmuir* **13**, 6058–6068.

Squires, T. M. & Brenner, M. P. 2000 Like-charge attraction and hydrodynamic interaction. *Phys. Rev. Lett.* **85**, 4976–4979.

Trau, M., Saville, D. A. & Aksay, I. A. 1997 Assembly of colloidal crystals at electrode interfaces. *Langmuir* **13**, 6375–6381.

Young, N. O., Goldstein, J. S. & Block, M. J. 1959 The motion of bubbles in a vertical temperature gradient. *J. Fluid Mech.* **6**, 350–356.